

Compressed Sensing Construction for Underdetermined Source Separation

Yujie Zhang^{1,2}  · Shizhong Zhang³ · Rui Qi^{3,4}

Received: 22 February 2016 / Revised: 8 February 2017 / Accepted: 10 February 2017 /
Published online: 6 March 2017
© Springer Science+Business Media New York 2017

Abstract Underdetermined blind source separation based on compressed sensing (CS) has already been proven to be an effective mechanism from an experimental viewpoint. In this study, we develop a theoretical result and show that, under a certain sparsity constraint for the restricted isometry property, the accuracy of CS when retrieving sources is guaranteed. This theoretical result can be regarded as a generalization of the blocked polynomial deterministic matrix theory and has been confirmed using numerical examples.

Keywords Underdetermined blind source separation · Compressed sensing · Restricted isometry property · Blocked matrix

1 Introduction

Underdetermined blind source separation (UBSS) is the process of restoring a set of unknown source signals from their linear instantaneous mixture. The problem can be described as follows:

✉ Yujie Zhang
zhangyujie@cug.edu.cn

Shizhong Zhang
sz_zhang2004@126.com

Rui Qi
qqr0425@163.com

¹ School of Mathematics and Physics, China University of Geosciences, Wuhan, China

² School of Computer Science, University of Windsor, Windsor, ON, Canada

³ Subsurface Multi-scale Imaging Lab, China University of Geosciences, Wuhan, China

⁴ School of Science, Naval University of Engineering, Wuhan, China

$$\mathbf{x}(t) = \mathbf{A}\mathbf{s}(t), \quad t = 1, 2, \dots, L, \quad (1)$$

where $\mathbf{x}(t) = [x_1(t), x_2(t), \dots, x_M(t)]^T$ and $\mathbf{s}(t) = [s_1(t), s_2(t), \dots, s_N(t)]^T$ are the observed and unknown source signals, respectively, and t is the discrete time sequence. $\mathbf{A} = (a_{ij})_{M \times N} \in \mathbb{R}^{M \times N}$ represents an unknown mixing matrix assumed to be row full rank, L is the length of the signals, and $M < N \ll L$. In UBSS, identification of the mixing matrix and restoration of the sources are two distinct problems. For linear memoryless mixture models (1), even if the mixing matrix is perfectly known, there exist infinite solutions [10]. In addition, priors are necessary to restore sources. Sparse signal representation is an effective method, requiring sources that are sparse or can be decomposed into a combination of sparse components [15, 21]. Sparsity of source signals implies that, in each column of \mathbf{s} , only a few significant values (active sources) exist, whereas most of the other elements are almost zero (inactive sources).

Compressed sensing (CS) is a new framework for signal recovery that has attracted considerable interest over the past few years [6, 23]. This framework assumes that the signal is sparse or compressible.

The CS model can be described as follows:

$$\mathbf{y} = \Phi\boldsymbol{\theta}, \quad (2)$$

where Φ denotes the $M_1 \times N_1$ ($M_1 < N_1$) matrix known as the measurement matrix. Although reconstruction of the signal $\boldsymbol{\theta}$ from \mathbf{y} is an ill-posed problem, prior knowledge of signal sparsity allows recovery of $\boldsymbol{\theta}$ from only $M_1 = O(K \log N_1)$ samples [2].

The search for a solution with minimal l_0 -norm, i.e., minimum number of nonzero components, is a natural and straightforward reconstruction method. However, this l_0 -norm minimization problem tends to become intractable as the dimension increases. It is also very sensitive to noise, and cannot be used for practical applications [2]. To overcome these severe drawbacks in signal recovery, significant attention is given to a family of algorithms that include thresholding [18], orthogonal matching pursuit (OMP) [14], stagewise OMP (StOMP) [5], regularized OMP (ROMP) [12], compressive sampling matching pursuit (CoSaMP) [11], subspace pursuit (SP) [21], basis pursuit principle [19], and generalized OMP (gOMP) [16]. To recover sources successfully, all of these approaches require that the measurement matrices Φ follow a uniform uncertainty principle, where each submatrix of Φ has to be well designed to satisfy the restricted isometry property (RIP) with a constant parameter [2, 17]. A measurement matrix Φ satisfies the RIP of order K if there exists a constant $\delta_K \in (0, 1)$ such that

$$(1 - \delta_K) \|\boldsymbol{\theta}\|_2^2 \leq \|\Phi\boldsymbol{\theta}\|_2^2 \leq (1 + \delta_K) \|\boldsymbol{\theta}\|_2^2, \quad \boldsymbol{\theta} \in \Sigma_K, \quad (3)$$

for any K -sparse vector $\boldsymbol{\theta}$. In particular, the minimum of all constants δ_K satisfying model (3) is called the restricted isometry constant, denoted by $\delta_K(\Phi)$.

Various measurement matrices have been investigated in recent years. The first family of measurement matrices consisted of the random Gaussian matrix, Bernoulli matrix, sub-Gaussian matrix, and basis transformation [8]. Although these matrices

each have their own unique advantages, their common drawback is that they are random matrices. In source separation, the measuring system is not normally under our control.

Beginning from the RIP conditions of model (2), the bound on $\delta_K(\Phi)$ was given in [1]. Then, the CS methods reported in [20, 22] can be used to recover the sources efficiently when the UBSS model is interleaved with the CS model. These methods have demonstrated good performance when validated via numerical experiments. However, use of CS methods in the UBSS model (1) is not clearly elucidated.

In 2007, a polynomial deterministic matrix method was proposed for compressed sensing [3]. The method affords good reconstruction properties similar to the Gaussian random matrix, but the number of measurements is inflexible [9]. Therefore, the blocked polynomial deterministic matrix was constructed in [9]. However, when the CS method is applied to the UBSS model, the measurement matrix does not meet the requirements of a blocked polynomial deterministic matrix, i.e., that the elements be either 0 or 1, rendering this method inapplicable to UBSS.

In this study, we extend the result from the blocked polynomial deterministic matrix to a more general case without any restriction on the elements of the matrix. Consequently, \mathbf{A} is assumed to be known.

The remainder of this paper is organized as follows: In Sect. 2, we discuss the UBSS and CS models, present the construction of the measurement matrix, and describe the notations used herein. In Sect. 3, we illustrate the proof of a theorem that the measurement matrix must satisfy. In Sect. 4, the proposed algorithm for sparse signal recovery is presented. Section 5 presents the simulation results, and concluding remarks are presented in Sect. 6.

2 UBSS and CS

2.1 Notations

The notations used in this study are as follows:

$\|\cdot\|_p$ denotes the l_p -norm.

$\#(\Gamma)$ denotes the number of elements in set Γ .

$$\boldsymbol{\theta}_i = [s_1(i), s_2(i), \dots, s_N(i)]^T, \quad i = 1, 2, \dots, L.$$

Σ_K denotes the set of all vectors $\mathbf{s} \in R^N$ such that at most K coordinates of \mathbf{s} are nonzero.

$\Gamma_i \subset \{(i-1)N+1, (i-1)N+2, \dots, iN\}$ denotes the set corresponding to $\boldsymbol{\Pi}_i$ and $\#(\Gamma_i) = K_i$.

$\boldsymbol{\Pi}_{\Gamma_i}$ represents the $M \times K_i$ matrix formed by the columns of $\boldsymbol{\Pi}_i$ with indices from Γ_i .

2.2 Relationship between UBSS and CS

The UBSS problem can be formulated as a compressed sensing model when the mixing matrix $\mathbf{A} = (a_{ij})_{M \times N}$ is known.

The relationship between UBSS and compressed sensing becomes evident if we interleave observations and sources into vectors as follows:

$$\mathbf{y} = [x_1(1), \dots, x_M(1), x_1(2), \dots, x_M(2), \dots, x_1(L), \dots, x_M(L)]^T \quad (4)$$

and

$$\boldsymbol{\theta} = [s_1(1), \dots, s_N(1), s_1(2), \dots, s_N(2), \dots, s_1(L), \dots, s_N(L)]^T. \quad (5)$$

Then, the mixing system in Eq. (1) can be expressed as

$$\mathbf{y} = \boldsymbol{\Pi}\boldsymbol{\theta}. \quad (6)$$

This is identical to the compressed sampling measurement equation

$$\boldsymbol{\Pi} = \begin{pmatrix} \mathbf{A} & \mathbf{0} & \dots & \mathbf{0} \\ \mathbf{0} & \mathbf{A} & \dots & \mathbf{0} \\ \vdots & \vdots & \ddots & \vdots \\ \mathbf{0} & \mathbf{0} & \dots & \mathbf{A} \end{pmatrix}_{ML \times NL} \doteq \begin{pmatrix} \boldsymbol{\Pi}_1 & \mathbf{0} & \dots & \mathbf{0} \\ \mathbf{0} & \boldsymbol{\Pi}_2 & \dots & \mathbf{0} \\ \vdots & \vdots & \ddots & \vdots \\ \mathbf{0} & \mathbf{0} & \dots & \boldsymbol{\Pi}_L \end{pmatrix}, \quad (7)$$

where $\boldsymbol{\Pi}_i$ denotes the i -th matrix \mathbf{A} in $\boldsymbol{\Pi}$.

2.3 Deterministic Construction of Matrix

To understand this property better, we first review some of the important results of the compressed sensing model (2) using the RIP in [2, 17]. Consider the $M \times \#\Gamma$ matrices $\boldsymbol{\Phi}_\Gamma$ formed by the columns of $\boldsymbol{\Phi}$ with indices from Γ , where $\Gamma \subseteq \{1, 2, \dots, N_1\}$. Then, Eq. (3) shows that the Gramian matrices

$$\mathbf{B}_\Gamma = \boldsymbol{\Phi}_\Gamma^T \boldsymbol{\Phi}_\Gamma, \#\Gamma = K \quad (8)$$

are bounded on the l_2 -norm and are uniform for all Γ such that $\#\Gamma = K$ [3]. The matrix \mathbf{B} is nonnegative definite and symmetric, i.e., has eigenvalues in $[1 - \delta_K, 1 + \delta_K]$:

$$1 - \delta_K \leq \| \mathbf{B}_\Gamma \|_2 \leq 1 + \delta_K. \quad (9)$$

A deterministic construction of matrices that satisfy the RIP is presented in [3].

Theorem 1 *Let $\boldsymbol{\Phi}_0$ be an $M_1 \times N_1$ matrix with columns v_Q , $Q \in P_r$ with the columns ordered lexicographically with respect to the coefficients of the polynomials and $M_1 = p^2$, $N_1 = p^{r+1}$. Then, the matrix $\boldsymbol{\Phi} = \frac{1}{\sqrt{p}} \boldsymbol{\Phi}_0$ satisfies the RIP with $\delta = \frac{(k-1)r}{p}$ for any $k < \frac{p}{r} + 1$, where P_r denotes the set of polynomials of degree $\leq r$, ($0 < r < p$) on finite fields, making any polynomial $Q(x) = b_0 + b_1x + \dots + b_r x^r \in P_r$, where b_0, b_1, \dots, b_r are the coefficients [3].*

In this theorem, the size and value of Φ are fixed, which is not feasible for practical applications. In the next section, we extend this theoretical result to the general case. The size and value of Φ are more flexible, and this result can be applied to UBSS.

3 Theoretical Result for UBSS Based on CS

In UBSS, it is assumed that each signal $s(t) \in R^N, t = 1, 2, \dots, L$ can be sparsely represented by K (usually $K \ll N$) or fewer nonzero (significant) components. For simplicity but without loss of generality, in this study, $s(t)$ is considered to be sparse in the time domain.

Here, three assumptions are presented:

- (i) The columns of \mathbf{A} are normalized, i.e., $\sum_{i=1}^M a_{ij}^2 = 1, j = 1, 2, \dots, N$, and any $M \times M$ submatrix of the mixing matrix \mathbf{A} is full rank [4, 7].
- (ii) The sparsity of θ , as defined in Eq. (5), is K , and the sparsity of $s_i(t)$ is $K_i, i = 1, 2, \dots, L$, which implies that $\sum_{i=1}^L K_i = K$.
- (iii) Let $q = \max_{i \in \{1, 2, \dots, L\}} (K_i)$ and Θ be the index set of arbitrarily chosen q columns from \mathbf{A} . We suppose that $\sum_{i_1, i_2 \in \Theta, i_1 \neq i_2} \langle \mathbf{a}_{i_1}, \mathbf{a}_{i_2} \rangle < 1$, where \mathbf{a}_k represents the k -th column of \mathbf{A} .

We now provide a deterministic construction of matrices that satisfy the RIP in UBSS.

Theorem 2 *Let $\mathbf{\Pi}$ denote a matrix constructed according to Eq. (7) that satisfies assumptions (i), (ii), and (iii). If*

$$\delta_i = (K_i - 1) \max_{k, h \in \Gamma_i, k \neq h} \{\mathbf{D}_\Gamma(k, h)\} < 1, \tag{10}$$

where $\mathbf{D}_\Gamma(k, h)$ is the k -th row and h -th column element of the Gramian matrix of $\mathbf{\Pi}_\Gamma$, which represents an $ML \times K$ matrix formed by the K columns of $\mathbf{\Pi}$, then matrix $\mathbf{\Pi}$ satisfies the RIP with $\delta = \max_{i=1, 2, \dots, L} \delta_i$.

Proof The proof is given in the Appendix.

Remark 1 The RIP is a sufficient condition to guarantee that matrix Φ has good source recovery performance.

Remark 2 The RIP is a condition on the spectral norm of matrices $\mathbf{D}_\Gamma = \mathbf{\Pi}_\Gamma^T \mathbf{\Pi}_\Gamma$. We have bounded the spectral norm by bounding the l_1 - and l_∞ -norms. Direct estimation of the spectral norm may lead to a stronger result than that of the l_1 - and l_∞ -norms.

4 Algorithm

In this section, we summarize the algorithm process, which involves two main steps. First, it judges whether the measurement matrix satisfies the RIP based on Theorem 2, then it uses the OMP algorithm to reconstruct the sources. The algorithm can be outlined as follows:

Algorithm

Input: Mixing matrix \mathbf{A} ; the total sparsity K ; observed signals \mathbf{X} .

Step 1: Transfer the observed signals \mathbf{X} into $\tilde{\mathbf{X}}$ in some transform domain using linear transformation (such as Fast Fourier Transform (FFT)), $\tilde{\mathbf{X}} = FFT(\mathbf{X})$.

Step 2: Transform the sparse signals to a column vector

$$\mathbf{y} = [\tilde{x}_1(1), \dots, \tilde{x}_M(1), \tilde{x}_1(2), \dots, \tilde{x}_M(2), \dots, \tilde{x}_1(L), \dots, \tilde{x}_M(L)]^T.$$

Step 3: Obtain the measurement matrix $\mathbf{\Pi}$ by Eq. (7).

Step 4: Use the OMP algorithm to find the sparsest coefficients [15], $\hat{\boldsymbol{\theta}} = OMP(\mathbf{y}, \mathbf{\Pi}, K)$.

Step 5: Split the resultant single vector $\hat{\boldsymbol{\theta}}$ into multiple source $\tilde{\hat{\mathbf{s}}}_i, i = 1, 2, \dots, N$ vectors by Eq.(5).

Step 6: Compute an inverse transform of these coefficients $\tilde{\hat{\mathbf{s}}}_i, i = 1, 2, \dots, N$ to obtain the estimations of the original sources, $\hat{\mathbf{s}}_i = IFFT(\tilde{\hat{\mathbf{s}}}_i), i = 1, 2, \dots, N$.

Output: $\hat{\mathbf{s}}_i, i = 1, 2, \dots, N$.

5 Simulation Results

Two experiments were performed to evaluate the effect of the algorithm on the separation performance relative to the shortest path method [21]. These two experiments show the recovery capability in the time and frequency domains for different sizes.

To evaluate the reconstruction results, the signal-to-interference ratio (SIR) was defined as a reconstruction index [7],

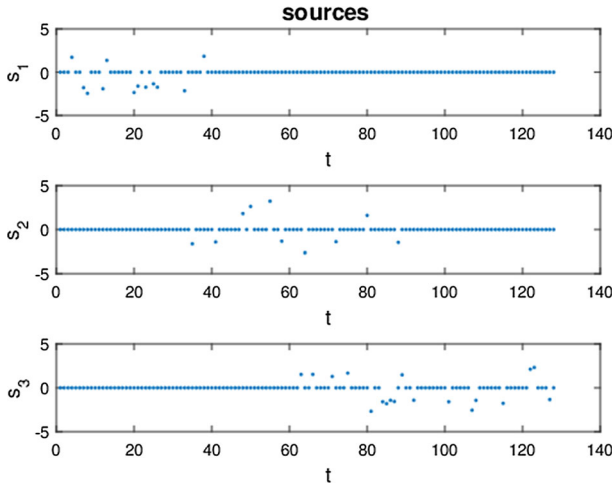


Fig. 1 Three source signals s_1, s_2, s_3

$$SIR_i = 10 \log_{10} \left(\frac{\sum_{t=1}^L s_i^2(t)}{\sum_{t=1}^L (\hat{s}_i(t) - s_i(t))^2} \right), \quad i = 1, 2, \dots, N, \quad (11)$$

where s_i is the source signal and \hat{s}_i is the corresponding reconstructed signal. This means that, the larger the SIR, the better the performance of the algorithm.

Experiment 1 $M = 2, N = 3, \max(k_i) = 2$.

In this experiment, we considered a blind source separation scenario with $M = 2$ mixtures and $N = 3$ source signals s_1, s_2, s_3 , which means that the dimension of the mixing matrix \mathbf{A} is 2×3 . Three sparse source signals were generated with length of $L = 128, \max(K_i) = 2$. The waveforms of the three original signals are shown in Fig. 1.

The mixing matrix is as follows:

$$\mathbf{A} = \begin{bmatrix} 0.8192 & 0.6727 & 0.4657 \\ 0.5735 & 0.7399 & 0.8849 \end{bmatrix},$$

where \mathbf{A} was randomly generated, normalized, and known when generated in the experiment. The detailed process to generate the matrix was as follows: First, we randomly generated a matrix $\mathbf{A}' = (a'_{ij})_{M \times N}$, then we normalized matrix \mathbf{A}' to $\mathbf{A} = (a_{ij})_{M \times N}$ s.t. $\sum_{i=1}^M a_{ij}^2 = 1, j = 1, 2, \dots, N$. Note that any $M \times M$ submatrix of the mixing matrix \mathbf{A} is full rank.

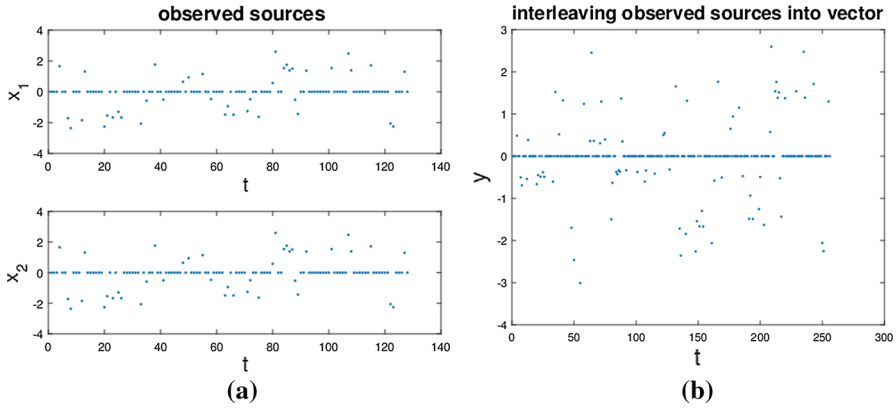


Fig. 2 Waveforms of observed signals: **a** waveforms of observed signals x_1, x_2 based on Eq. (1), **b** waveform after transforming the observed sources into a column vector y

Figure 2a shows the waveform of the observed signals. The observed signals were then interleaved into a column vector as indicated in Eq. (4). The waveform is displayed in Fig. 2b.

According to Theorem 2, we computed $A^T A$ as follows:

$$G = A^T A = \begin{bmatrix} 1.0000 & 0.9754 & 0.8890 \\ 0.9754 & 1.0000 & 0.9681 \\ 0.8890 & 0.9681 & 1.0000 \end{bmatrix}.$$

Then, the off-diagonal entries $D_\Gamma(k, h) = G(k, h) < 1, k \neq h$, such that

$$\delta_i = (K_i - 1) \max_{k, h \in \Gamma_i, k \neq h} \{D_\Gamma(k, h)\} = 0.9754 < 1.$$

Therefore, the original sources can be estimated by using an appropriate CS algorithm. Figure 3a shows the separation results obtained by OMP. Then, the resultant single vector was split into multiple separation vectors, which are displayed in Fig. 3b.

We performed 100 trials to evaluate the reconstruction results. The average SIR was used to evaluate the reconstruction errors. Table 1 records the average SIR compared with the shortest path method, showing that UBSS based on OMP obtains results similar to those of the shortest path method when the measurement matrix satisfies Theorem 2.

Experiment 2 $M = 3, N = 4, \max(k_i) = 2$.

In practical applications, not all signals are sparse in the time domain, but they are sparse in transformed domains. In this experiment, we created four source signals, namely s_1, s_2, s_3, s_4 , that are not sparse in the time domain but are sparse in Fourier-transform domains $\tilde{s}_1, \tilde{s}_2, \tilde{s}_3, \tilde{s}_4$ with length $L = 128, M = 3, N = 4, \max(K_i) = 2$.

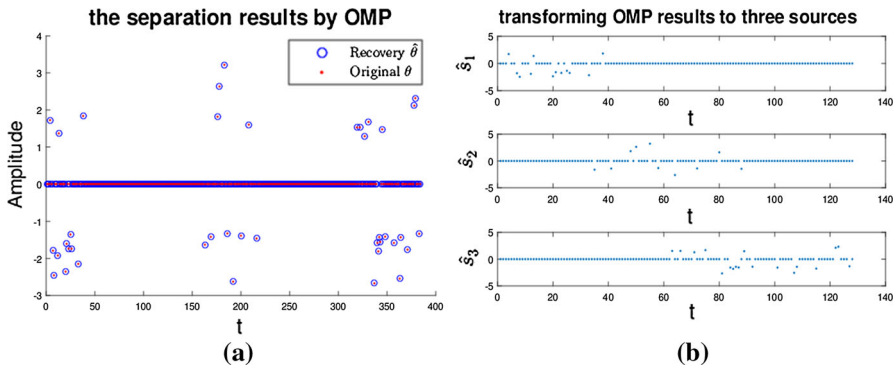


Fig. 3 Separation results: **a** separation results obtained by OMP (red dots original sources θ , blue circle corresponding estimations $\hat{\theta}$), **b** waveform after splitting the single vector $\hat{\theta}$ into multiple separation vectors $\hat{s}_1, \hat{s}_2, \hat{s}_3$. For color references in this figure, please refer to the online version of the paper (Color figure online)

Table 1 Average SIR of sources and separation signals in experiment 1

Algorithm	SIR ₁ (s_1, \hat{s}_1)	SIR ₂ (s_2, \hat{s}_2)	SIR ₃ (s_3, \hat{s}_3)
Shortest path method	310.4159	315.5370	317.8050
OMP	326.2705	318.7403	319.1313

The mixing matrix is as follows:

$$A = \begin{bmatrix} 0.8256 & 0.3828 & 0.4857 & 0.4053 \\ 0.2008 & 0.7021 & 0.0197 & 0.5610 \\ 0.5273 & 0.6004 & 0.8739 & 0.7218 \end{bmatrix},$$

which was randomly generated and normalized.

Fast Fourier transformation was applied to obtain a sparse representation of each signal. The waveforms of the four original signals and their corresponding FFT coefficients are shown in Fig. 4. Here, we deal with the real and imaginary parts using the OMP method. The inverse FFT method is then applied to the reconstructed data comprising the real and imaginary parts of the separation vectors. Figure 4a shows the source signals, Fig. 4b shows the spectrum of the sources with FFT, and Fig. 4c and d depict the real and imaginary parts of the FFT domains of the sources, respectively.

First, the real and imaginary parts of the FFT domains of the sources were interleaved into a column as indicated by Eq. (5). Corresponding scatterplots are shown in Fig. 5a, b.

Figure 6a shows the waveform of the observed signals. Then, the real and imaginary parts of the FFT domains of the observed signals were interleaved into a column vector as indicated in Eq. (4). The waveform is displayed in Fig. 6b, c.

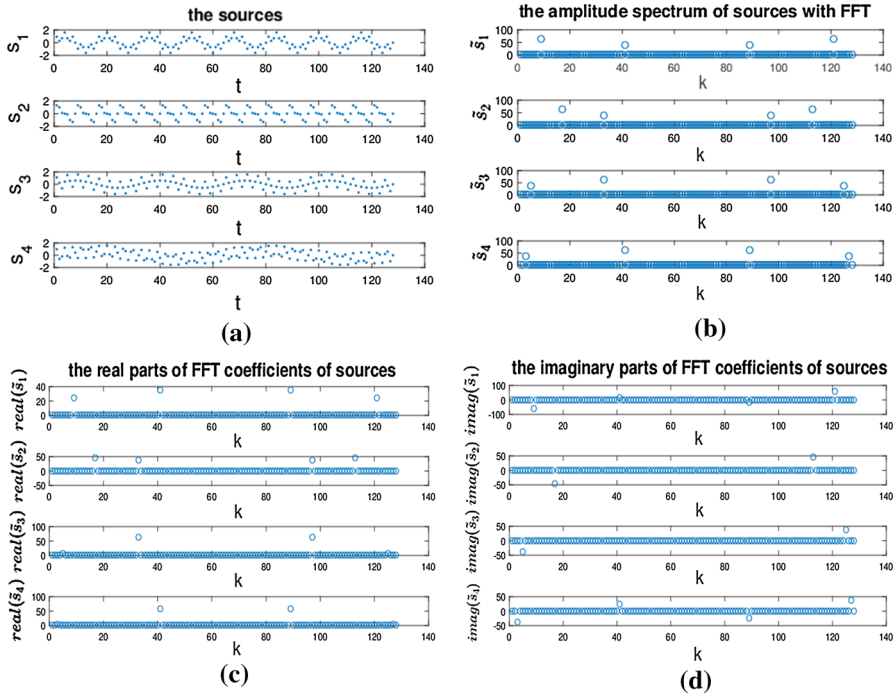


Fig. 4 Source signals and FFT coefficients: **a** source signals, **b** amplitude spectrum of sources with FFT, **c** real part of FFT domains of sources, and **d** imaginary part of FFT domains of sources. k stands for the number of FFT points

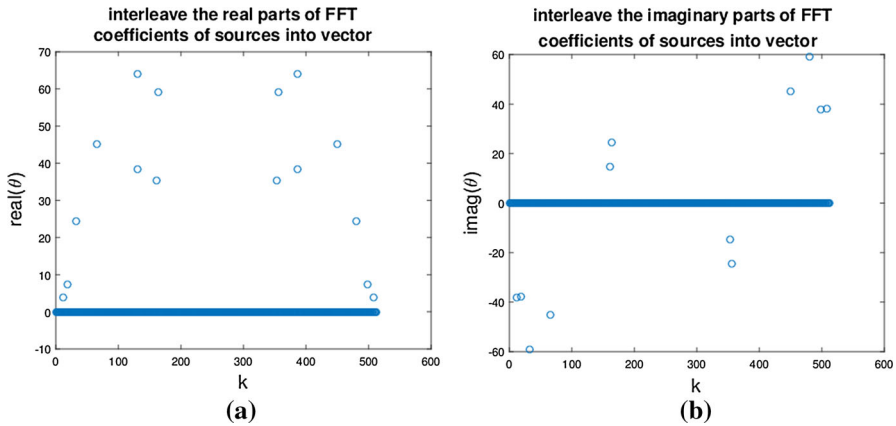


Fig. 5 Interleaving real and imaginary parts of FFT domains of source signals into a column: **a** interleaving the real parts of the FFT coefficients of sources into a column $real(\theta)$, **b** interleaving the imaginary parts of the FFT coefficients of sources into a column $imag(\theta)$. k stands for the number of FFT points

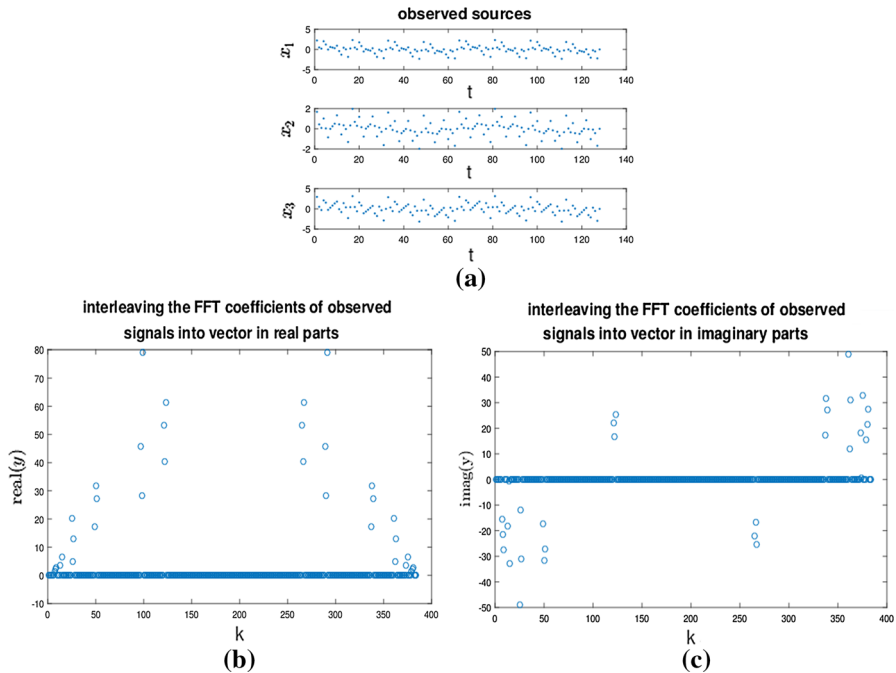


Fig. 6 Waveforms of observed signals and their real and imaginary parts of FFT domains: **a** the observed signals x_1, x_2, x_3 , **b** interleaving the FFT coefficients of observed signals into vectors with real part $real(y)$, **c** interleaving the FFT coefficients of observed signals into vectors with imaginary part $imag(y)$. k stands for the number of FFT points

According to Theorem 2, we computed $\mathbf{A}^T \mathbf{A}$ as follows:

$$\mathbf{G} = \mathbf{A}^T \mathbf{A} = \begin{bmatrix} 1.0000 & 0.7736 & 0.8658 & 0.8279 \\ 0.7736 & 1.0000 & 0.7245 & 0.9824 \\ 0.8658 & 0.7245 & 1.0000 & 0.8387 \\ 0.8279 & 0.9824 & 0.8387 & 1.0000 \end{bmatrix}.$$

Then,

$$\delta_i = (K_i - 1) \max_{k, h \in \Gamma_i, k \neq h} \{\mathbf{D}_\Gamma(k, h)\} = 0.9824 < 1.$$

Therefore, the real and imaginary parts of the FFT domains of the sources can be exactly reconstructed by using the OMP algorithm. Figure 7a and b present the separation results for the real and imaginary parts, respectively. All sparse representations were reconstructed properly.

The single vector was split into multiple separation vectors. Finally, the inverse FFT method was applied to the reconstructed data comprising the real and imaginary parts of the separation vectors, and the four original signals were recovered. The final results are shown in Fig. 8.

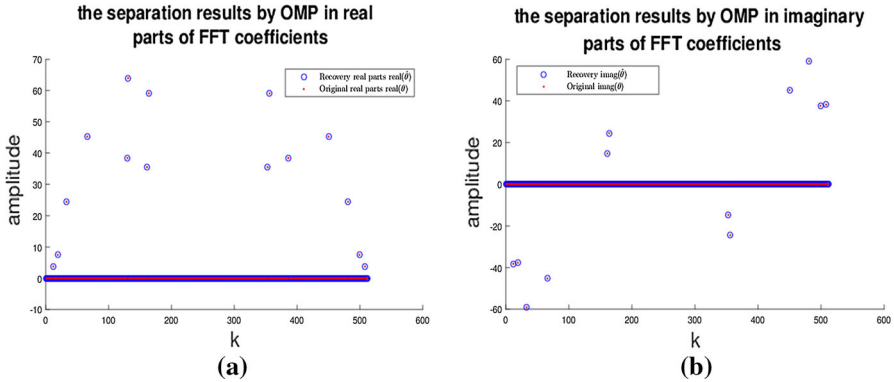


Fig. 7 Separation results using the OMP method for real and imaginary parts of FFT domains of observed signals: **a** separation results for real parts (*red dots* real parts $real(\theta)$ of original sources, *blue circle* corresponding real parts $real(\hat{\theta})$ of estimations), **b** separation results for imaginary parts (*red dots* imaginary parts $imag(\theta)$ of original sources, *blue circle* corresponding imaginary parts $imag(\hat{\theta})$ of estimations). k stands for the number of FFT points. For color references in this figure, please refer to the online version of the paper (Color figure online)

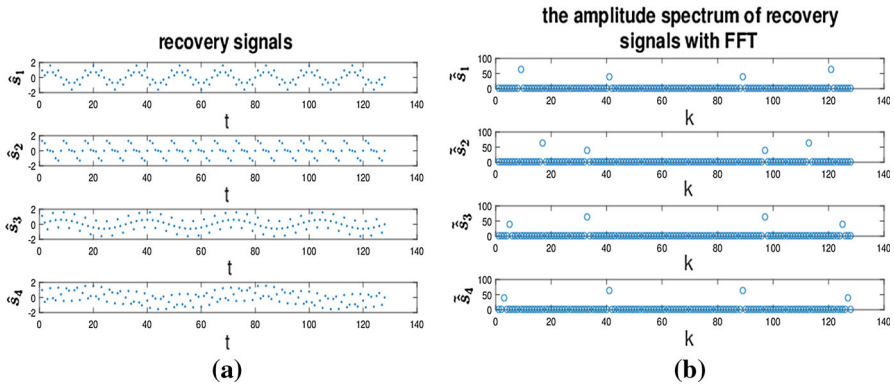


Fig. 8 Recovered signals and their FFT spectrum: **a** recovered signals $\hat{s}_1, \hat{s}_2, \hat{s}_3, \hat{s}_4$, **b** amplitude spectrum $\hat{s}_1, \hat{s}_2, \hat{s}_3, \hat{s}_4$ of the recovered signals with FFT. k stands for the number of FFT points

Table 2 Average SIR of sources and separation signals in experiment 2

Algorithm	SIR ₁ (s_1, \hat{s}_1)	SIR ₂ (s_2, \hat{s}_2)	SIR ₃ (s_3, \hat{s}_3)	SIR ₄ (s_4, \hat{s}_4)
Shortest path method	145.2400	131.8626	108.7379	139.1085
OMP	145.8967	144.9157	144.1111	142.2850

After 100 trials, the average SIR relative to that obtained using the shortest path method is recorded in Table 2, showing that UBSS based on OMP produced identical results for both the proposed method and the shortest path method when the measurement matrices satisfy Theorem 2.

6 Conclusions

Separation of underdetermined mixtures is usually addressed in the framework of sparse signal representation. In recent years, compressed sensing theory has been adopted for signals that permit a sparse representation. The major contribution of this paper is the extension of a recent theoretical result. Numerical experiments demonstrate the separation performance of the proposed theory. The result can be directly extended to higher-dimensional as well as dependent source separation.

However, there is a limitation to the proposed theory: The linear transform used to make the sources sparse and the maximum sparsity of all the blocks must be known a priori. Extending the proposed results to a more general case (such as when the separation of convolutive mixtures or the sparsity is unknown) is left for future work.

Acknowledgements This work was partially supported by the Natural Science Foundation of China under Grant No. 61601417. The authors would like to thank the anonymous reviewers for their thorough reading of the paper and patient feedback.

Appendix: Proof of Theorem 2

From Eq. (5), the length and sparsity of signal θ are NL and K , respectively. $\Gamma \in \{1, 2, \dots, NL\}$ and $\#(\Gamma) = K$. Without loss of generality, we assume that the source signals \mathbf{s} are sparse in the time domain, then the sparsity of θ_i is K_i . Then, the Gramian matrix can be written as follows:

$$\begin{aligned}
 \mathbf{D}_\Gamma &= \Pi_\Gamma^T \Pi_\Gamma = \begin{pmatrix} \Pi_{\Gamma_1} & \mathbf{0} & \cdots & \mathbf{0} \\ \mathbf{0} & \Pi_{\Gamma_2} & \cdots & \mathbf{0} \\ \vdots & \vdots & \ddots & \vdots \\ \mathbf{0} & \mathbf{0} & \cdots & \Pi_{\Gamma_L} \end{pmatrix}_{K \times ML}^T \begin{pmatrix} \Pi_{\Gamma_1} & \mathbf{0} & \cdots & \mathbf{0} \\ \mathbf{0} & \Pi_{\Gamma_2} & \cdots & \mathbf{0} \\ \vdots & \vdots & \ddots & \vdots \\ \mathbf{0} & \mathbf{0} & \cdots & \Pi_{\Gamma_L} \end{pmatrix}_{ML \times K} \\
 &= \begin{pmatrix} \Pi_{\Gamma_1}^T \Pi_{\Gamma_1} & \mathbf{0} & \cdots & \mathbf{0} \\ \mathbf{0} & \Pi_{\Gamma_2}^T \Pi_{\Gamma_2} & \cdots & \mathbf{0} \\ \vdots & \vdots & \ddots & \vdots \\ \mathbf{0} & \mathbf{0} & \cdots & \Pi_{\Gamma_L}^T \Pi_{\Gamma_L} \end{pmatrix}_{K \times K} \\
 &\doteq \begin{pmatrix} \mathbf{D}_{\Gamma_1} & \mathbf{0} & \cdots & \mathbf{0} \\ \mathbf{0} & \mathbf{D}_{\Gamma_2} & \cdots & \mathbf{0} \\ \vdots & \vdots & \ddots & \vdots \\ \mathbf{0} & \mathbf{0} & \cdots & \mathbf{D}_{\Gamma_L} \end{pmatrix}, \tag{12}
 \end{aligned}$$

where $\mathbf{D}_{\Gamma_i} = \Pi_{\Gamma_i}^T \Pi_{\Gamma_i}$; That is,

$$\mathbf{D}_\Gamma(k, h) = \langle \Pi_\Gamma(\cdot, k), \Pi_\Gamma(\cdot, h) \rangle = \sum_{j=1}^{ML} \Pi_\Gamma(j, k) \Pi_\Gamma(j, h). \tag{13}$$

From Eq. (12), we have

- (i) when $k, h \in \Gamma_i$
 - (a) if $k = h$, then $\mathbf{D}_\Gamma(k, k) = 1$;
 - (b) if $k \neq h$, $\mathbf{D}_\Gamma(k, h) = \sum_{j=1}^{ML} \Pi_\Gamma(j, k)\Pi_\Gamma(j, h) = \langle \mathbf{a}_{k'}, \mathbf{a}_{h'} \rangle$.
- (ii) when $k \in \Gamma_i, h \in \Gamma_j, i \neq j, \mathbf{D}_\Gamma(k, h) = 0$.

Because any off-diagonal entry of \mathbf{D}_Γ is less than $\max_{k \neq h} \{\mathbf{D}_\Gamma(k, h)\}$, the off-diagonal entries in any row or column of \mathbf{D}_Γ have sum

$$\delta_i \doteq (K_i - 1) \max_{k, h \in \Gamma_i, k \neq h} \{\mathbf{D}_\Gamma(k, h)\}. \text{ If } \delta_i < 1 \tag{14}$$

then

$$K_i = \frac{\delta_i}{\max_{k, h \in \Gamma_i, k \neq h} \{\mathbf{D}_\Gamma(k, h)\}} + 1. \tag{15}$$

Let $\delta = \max_{i=1,2,\dots,L} \delta_i < 1$, then

$$\begin{aligned} K &= \sum_{i=1}^L K_i = \sum_{i=1}^L \left(\frac{\delta_i}{\max_{k, h \in \Gamma_i, k \neq h} \{\mathbf{D}_\Gamma(k, h)\}} + 1 \right) \\ &\leq \sum_{i=1}^L \left(\frac{\delta}{\max_{k, h \in \Gamma_i, k \neq h} \{\mathbf{D}_\Gamma(k, h)\}} + 1 \right). \end{aligned} \tag{16}$$

Hence, we write

$$\mathbf{D}_\Gamma = \mathbf{I} + \mathbf{B}_\Gamma, \tag{17}$$

where \mathbf{I} is a unit matrix and

$$\| \mathbf{B}_\Gamma \|_p \leq \delta, \quad p = 1 \text{ or } p = \infty. \tag{18}$$

As \mathbf{B}_Γ is a symmetric matrix, by interpolation of operators, we obtain that

$$\| \mathbf{B}_\Gamma \|_2 = \rho(\mathbf{B}_\Gamma) \leq \| \mathbf{B}_\Gamma \|_p \leq \delta, \quad p = 1 \text{ or } p = \infty, \tag{19}$$

where $\rho(\mathbf{B}_\Gamma)$ denote the spectral norm of \mathbf{B}_Γ . Since $\| \mathbf{A} + \mathbf{B} \|_2 \leq \| \mathbf{A} \|_2 + \| \mathbf{B} \|_2$ for any matrices \mathbf{A} and \mathbf{B} [13], it follows that

$$\| \mathbf{D}_\Gamma \|_2 \leq 1 + \delta, \quad \| \mathbf{D}_\Gamma^{-1} \|_2 \leq (1 - \delta)^{-1}. \tag{20}$$

Therefore, \mathbf{D}_Γ has eigenvalues in $[1 - \delta, 1 + \delta]$. Therefore, we have proved that matrix $\mathbf{\Pi}$ satisfies the RIP with $\delta = \max_{i=1,2,\dots,L} \delta_i$.

References

1. T. Blumensath, M.E. Davies, Compressed sensing and source separation, in *Proceedings of the International Conference on Independent Component Analysis and Blind Source Separation*, pp. 341–348 (2007)
2. E. Candes, J. Romberg, T. Tao, Robust uncertainty principles: exact signal reconstruction from highly incomplete frequency information. *IEEE Trans. Inf. Theory* **52**(2), 489–509 (2006)
3. R.A. Devore, Deterministic constructions of compressed sensing matrices. *J. Complex.* **23**(4–6), 918–925 (2007)
4. T.B. Dong, Y.K. Lei, J.S. Yang, An algorithm for underdetermined mixing matrix estimation. *Neurocomputing* **104**, 26–34 (2013)
5. D.L. Donoho, Y. Tsaig, I. Drori, J.L. Starck, Sparse solution of underdetermined systems of linear equations by stagewise orthogonal matching pursuit. *IEEE Trans. Inf. Theory* **58**(2), 1094–1121 (2012)
6. A. Flinth, A geometrical stability condition for compressed sensing. *Linear Algebra Appl.* **504**, 406–432 (2016)
7. Z.Y. He, S.L. Xie, L. Zhang, A. Cichocki, A note on Lewicki–Sejnowski gradient for learning over-complete representation. *Neural Comput.* **20**(3), 636–643 (2008)
8. R. Holger, S. Karin, V. Pierre, Compressed sensing and redundant dictionaries. *IEEE Trans. Inf. Theory* **54**(5), 2210–2219 (2008)
9. X.B. Li, R.Z. Zhao, S.H. Hu, Blocked polynomial deterministic matrix for compressed sensing, in *Proceedings of the International Conference on Wireless Communications, Networking and Mobile Computing*, pp. 1–4 (2010)
10. F.M. Naini, H. Mohimani, M. Zadeh, C. Jutten, Estimating the mixing matrix in space component analysis based on partial k -dimensional subspace clustering. *Neurocomputing* **71**, 2330–2343 (2008)
11. D. Needell, J.A. Tropp, CoSaMP: iterative signal recovery from incomplete and inaccurate samples. *Appl. Comput. Harmon. Anal.* **26**(3), 301–321 (2008)
12. D. Needell, R. Vershynin, Signal recovery from inaccurate and incomplete measurements via regularized orthogonal matching pursuit. *IEEE J. Sel. Top. Signal Process.* **4**(2), 310–316 (2010)
13. R.C. Shi, F. Wei, *Matrix Analysis*, 2nd edn. (Beijing Institute of Technology Press, Beijing, 2008)
14. A.G. Shwetha, V.S. Saroja, Compressed sensing reconstruction of an audio signal using OMP. *Int. J. Adv. Comput. Res.* **5**(18), 75–79 (2015)
15. Y.C. Sun, J. Xin, Underdetermined sparse blind source separation of nonnegative and partially overlapped data. *SIAM J. Sci. Comput.* **33**(4), 2063–2094 (2011)
16. J. Wang, S. Kwon, B. Shim, Generalized orthogonal matching pursuit. *IEEE Trans. Signal Process.* **60**(12), 6202–6216 (2012)
17. J. Wang, S. Kwon, P. Li, B. Shim, Recovery of sparse signals via generalized orthogonal matching pursuit: a new analysis. *IEEE Trans. Signal Process.* **64**(4), 1076–1089 (2016)
18. K. Wei, Fast iterative hard thresholding for compressed sensing. *IEEE Signal Process. Lett.* **22**(5), 593–597 (2015)
19. Y.J. Xie, Y.F. Ke, C.F. Ma, The modified accelerated Bergman method for regularized basis pursuit problem. *J. Inequal. Appl.* **2014**(1), 1–17 (2014)
20. T. Xu, W.W. Wang, A compressed sensing approach for underdetermined blind audio source separation with sparse representation, in *Proceedings of the IEEE International Workshop on Statistical Signal Processing*, pp. 493–496 (2009)
21. J.D. Xu, X.C. Yu, D. Hu, L.B. Zhang, A fast mixing matrix estimation method in the wavelet domain. *Signal Process.* **95**, 58–66 (2014)
22. T. Xu, W.W. Wang, A block-based compressed sensing method for underdetermined blind speech separation incorporating binary mask, in *Proceedings of the IEEE International Conference on Acoustics, Speech and Signal Processing (ICASSP2010)*, pp. 2022–2025 (2010)
23. E. Yonina, K. Gitta, *Compressed Sensing Theory and Applications* (Cambridge University Press, Cambridge, 2012)